Available online at www.sciencedirect.com
SCIENCE DIRECT®
Journal of Solid State Chemistry 178 (2005) 3265–3274
JOURNAL OF SOLID STATE CHEMISTRY
www.elsevier.com/locate/jssc

New binary systems Mg–*M*–O (*M* = Y, La, Ce): Synthesis and physico-chemical characterization

A.S. Ivanova*, B.L. Moroz, E.M. Moroz, Yu.V. Larichev, E.A. Paukshtis, V.I. Bukhtiyarov

Boreskov Institute of Catalysis SB RAS, Pr. Akad. Lavrentieva, 5, 630090 Novosibirsk, Russia

Received 31 May 2005; received in revised form 4 August 2005; accepted 4 August 2005
Available online 12 September 2005

Abstract

New binary oxide Mg–*M*–O (*M* = Y, La, Ce) systems are obtained by co-precipitation and characterized by adsorption methods, X-ray diffraction method (XRD), X-ray photoelectron spectroscopy (XPS) and Fourier transform infrared (FTIR) spectroscopy of adsorbed probe molecules (CO and $CDCl_3$). It is shown that Mg–Y–O systems after calcination at 450–750 °C represent the physical mixtures of MgO and Y_2O_3, while the components of Mg–La(Ce)–O systems interact to form La_2MgO_x and $(Ce,Mg)O_2$ solid solutions, respectively. From XPS data, the surface of the binary systems is enriched with lanthanide ions. Addition of ≈5 mol% M_2O_3 to MgO results in an increase in concentrations of strong and weak Lewis acidic sites, the content of the latter being much higher and changing in the series: MgO < Mg–Ce–O < Mg–La–O < Mg–Y–O. At the same time basic sites become stronger in the binary systems but their total content decreases in comparison to that in individual MgO. Mg–*M*–O samples containing ≈5 mol% M_2O_3 are highly-dispersed and characterized by bimodal porous texture.

Keywords: Binary systems Mg–*M*–O (*M* = Y, La, Ce); Synthesis; Bulk and surface structural parameters; Acid–base properties

1. Introduction

The systems based on alkaline and rare earth metal oxides have attracted recently much attention of researchers who consider them as promising catalysts and catalyst supports for a number of chemical reactions. For example, magnesia reveals a relatively high basicity that makes it an appropriate catalyst for oxidative condensation of hydrocarbons [1–3], synthesis of acrylonitrile from ethanol and acetonitrile [4], and hydrogenation of unsaturated ketones [5], as well as a support for Ru catalyst for ammonia synthesis [6–10]. With regard to the values of cation electronegativities (E_f) [11], Y(III), La(III) and Ce(III) oxides are stronger bases than MgO. Therefore, synthesis of binary MgO-based systems promoted with lanthanide oxides is of interest.

In the present work, binary oxide Mg–*M*–O (*M* = Y, La, Ce) systems were obtained for the first time; their chemical and phase compositions as well as specific surface areas depending on the nature of *M* and calcination temperature (T_{calc}) were determined. The surface composition and acid–base properties of Mg–*M*–O were characterized by means of X-ray photoelectron spectroscopy (XPS) measurements and Fourier transform infrared (FTIR) spectroscopy of adsorbed probe molecules.

2. Experimental

Samples of Mg–*M*–O (*M* = Y, La, Ce) were precipitated from a mixture of aqueous solutions of $Mg(NO_3)_2$ and $M(NO_3)_3$ (taken in a required

*Corresponding author. Fax: +7 383 3 308056.
E-mail address: iva@catalysis.nsk.su (A.S. Ivanova).

0022-4596/$ - see front matter © 2005 Published by Elsevier Inc.
doi:10.1016/j.jssc.2005.08.001

proportion) with 2 N KOH solution at pH 9.9 (±0.1) and temperature (T) 50±2 °C. The resulting suspension was allowed to stay for 2 h at these pH and T and then filtered; the precipitate was thoroughly washed with distilled water from nitrate impurity. The samples thus obtained were dried first in air at room temperature then in a drying oven at 110 °C for 12–14 h and calcined at 450 or 750 °C for 4 h in flowing air which was purified from moisture and CO_2 traces by passage through the column filled with active alumina.

Pure MgO, $Y(La)_2O_3$, and CeO_2 were prepared the same way by adding 2 N KOH solution to the metal nitrate solution.

The lanthanide content in the binary Mg–M–O systems was determined by atomic absorption spectrometry [12].

X-ray diffraction (XRD) experiments were conducted on a HZG-4C diffractometer using CuK_α monochromatic radiation. The XRD patterns were analyzed by means of PCW.2.4, Origin and Polycrystal computer programs [13,14]. The phase analysis was carried out by PCW.2.4 program by comparison of the experimental XRD patterns with the diffraction patterns which were theoretically calculated based on the known structures from ICDS database [15], a XRD peak profile having been taken into account at that. A XRD peak profile was fitted using PsevdoViot2 function represented a combination of the Gaussian and Lorentzian functions [16]. The parameters of XRD peak profile were refined to the best correspondence between the experimental XRD peak profile and the theoretically calculated one. The integral intensities and integral half-widths of XRD peaks were determined after refinement of the parameters of peak profile. The values of d_{hkl} found for the individual phases were used for least-squares refinement their cell parameters to ±0.003 Å. The size of mixed-oxide crystallites, D was calculated from XRD data by the Scherrer formula [17].

XPS were recorded on a VG ESCALAB HP spectrometer with AlK_α non-monochromatic radiation ($E_{h\nu}$ = 1486.6 eV, 200 W power). The binding energy (E_b) was calibrated, using the peaks of Au $4f_{7/2}$ (E_b = 84.0 eV) and Cu $2p_{3/2}$ (E_b = 932.6 eV). Charging was corrected using the Mg2s peak (E_b = 88.1 eV) as the internal standard. The E_b values and intensities were calculated after a Shirley-type background [18] was subtracted from raw photoemission spectra and an XP peak profile was fitted using a combination of the Gaussian and Lorentzian functions at their varied ratio. The surface contents of the elements were calculated from the related XP peak area, using the atomic sensitivity factors. For XPS study, the samples were pressed into a Ni grid, transferred to a test chamber and outgassed at 1–5 × 10^{-8} mbar and 450 °C for 1 h before the spectra registration.

Acid–base properties of surfaces of Mg–M–O systems were estimated by means of FTIR spectroscopy with adsorbed probe molecules (CO, $CDCl_3$) [19]. FTIR spectra were recorded using a Shimadzu 8300 FT spectrometer in the region of 1200–4000 cm^{-1} at the resolution of 4 cm^{-1}; the number of scans was equal to 50. The samples were pressed into self-supporting disks of 8–20 mg cm^{-2}, transferred to an IR cell and then evacuated at 450 °C for 2 h to residual pressure of $<10^{-4}$ Torr. Carbon monoxide was adsorbed at −196 °C and pressure ranged from 0.1 to 10 Torr. Adsorption of deuterochloroform was carried out at 0 °C and the pressure equal to $CDCl_3$ vapor pressure at 20 °C. The concentrations of various surface sites were calculated from integrated intensities of the characteristic absorption bands using the following integral extinction coefficients (k_i): k_i = 4.5 cm μmol^{-1} for OH groups with ν(OH) = 3756 cm^{-1}; k_i, = 0.8 and 0.65 cm μmol^{-1} for the complexes of Lewis acidic sites with CO, which are characterized by the bands at ν_{CO} = 2190–2196 and 2163–2177 cm^{-1}, respectively; k_i = 1.5, 1.0 and 0.8 cm μmol^{-1} for the complexes of basic sites with $CDCl_3$, which are characterized by the bands at ν_{CD} = 2160–2180, 2210–2230 and 2230–2238 cm^{-1}, respectively. The concentrations of surface sites were determined at the accuracy of ±25%.

The specific surface area of Mg–M–O systems was determined using heat desorption of argon [20] at an error of ±10%; the textural parameters were calculated from isotherms of low temperature (–196 °C) N_2 adsorption obtained using a Micromeritics ASAP-2400 instrument.

3. Results and discussion

The data on chemical and phase composition of Mg–M–O systems, as well as the values of the specific surface area are given in Table 1.

3.1. Phase composition

According to XRD method, the Mg–M–O systems newly obtained contain mainly two phases. In addition to the phase of magnesia, each of them involves either lanthanide oxide or a product of its interaction with MgO.

The Mg–Y–O sample containing 5 mol% of Y_2O_3 which had been calcined in flowing air at 450 °C represents a mixture of non-identified amorphous phase and the phase of MgO with an expanded unit cell parameter, a (Table 1). An increase in the Y_2O_3 content up to 17.5 mol% favors the crystallization of not only magnesia but also of yttria phase. In this case, the value of a determined for MgO in the Mg–Y–O sample agrees closely with the reference value for pure MgO

Table 1
Characteristics of the prepared binary Mg–*M*–O (*M* = Y, Ce, La) systems

Nos.	System	Content of M_2O_3, mol%		Phase composition after calcination at the given temperature[a]		Surface area after calcination at the given temperature, $m^2 g^{-1}$	
		Calc.	Found	$T_{calc} = 450\ ^\circ C$	$T_{calc} = 750\ ^\circ C$	$T_{calc} = 450\ ^\circ C$	$T_{calc} = 750\ ^\circ C$
1	Mg–Y–O	5.0	5.6	MgO: $a = 4.233$ Å, $D \sim 100$ Å; amorphous phase	MgO: $a = 4.216$ Å, $D = 160$ Å; Y_2O_3: $a = 10.613$ Å, $D = 115$ Å	210	115
2		10.0	8.1	Not determined	Not determined	145	97
3		25.0	17.5	MgO: $a = 4.211$ Å, $D = 250$ Å; Y_2O_3: $a = 10.701$ Å, $D = 25$ Å	MgO: $a = 4.211$ Å, $D = 250$ Å; Y_2O_3: $a = 10.610$ Å, $D = 125$ Å	105	95
4	Mg–La–O	5.0	4.1	Amorphous phase	MgO:$a = 4.211$ Å, $D = 250$ Å; La_2O_3: $D = 550$ Å; La_2MgO_x : $D = 250$ Å	220	113
5		10.0	7.3	Not determined	Not determined	200	105
6		25.0	14.3	Amorphous phase	MgO: $a = 4.212$ Å, $D = 200$ Å; La_2O_3: $a = 3.937$ Å; $c = 6.129$ Å; $D = 330$ Å; $La(OH)_3$: $a = 6.528$; $c = 3.858$ Å; $D = 290$ Å	105	48
7	Mg–Ce–O	5.0	5.7	MgO: $a = 4.231$ Å, $D = 100$ Å; $(Ce,Mg)O_2$: $a = 5.403$ Å; $D = 70$ Å	MgO: $a = 4.218$ Å, $D = 215$ Å; $(Ce,Mg)O_2$: $a = 5.406$ Å; $D = 220$ Å	230	95
8		10.0	9.1	Not determined	Not determined	170	98
9		25.0	23.0	MgO: $a = 4.218$ Å, $D = 80$ Å; $(Ce,Mg)O_2$: $a = 5.391$ Å; $D = 65$ Å	MgO: $a = 4.218$ Å, $D = 150$ Å; $(Ce,Mg)O_2$: $a = 5.403$ Å; $D = 210$ Å	104	85

[a]Designations: *a* and *c*—the unit cell parameters; *D*—the phase crystallite size.

($a = 4.211$ Å) whereas a value found of Y_2O_3 phase is considerably larger than the reference value ($a = 10.604$ Å) [15]. The Mg–La–O systems after calcination at 450 °C remain X-ray amorphous regardless of the La_2O_3 content. The Mg–Ce–O samples calcined at the same temperature represent a mixture of MgO and CeO_2 (Fig. 1) the values of a being larger for MgO phase but smaller for CeO_2 phase in comparison with the reference values. Since the value of a equals 5.411 Å for pure CeO_2 [15] but as low as 5.403 Å for MgO phase in the Mg–Ce–O samples, it is reasonable to suppose that a ceria-based solid solution, $(Ce,Mg)O_2$, is formed in the Mg–Ce–O systems.

An increase in T_{calc} to 750 °C promotes the crystallization of the amorphous phase in the Mg–La–O system with the formation of MgO, La_2O_3, and La_2MgO_x solid solution, as well. The phase composition of the Mg–Y(Ce)–O systems does not alter with T_{calc} increasing, but only the sintering of the constituent phases is observed (Table 1). Thus, XRD indicates that among the binary oxide systems under consideration the interaction between the constituents takes place in the Mg–La(Ce)–O systems and is absent in the Mg–Y–O system. That may be accounted for by the position of the lanthanide cations in the electronegativity series [11]: the difference in E_f is no more than 0.16 for Y^{3+} and Mg^{2+} cations but as large as 0.74 and 3.42 for La^{3+} and Mg^{2+} or for Ce^{4+} and Mg^{2+}, respectively.

As the lanthanide content increases in the binary Mg–M–O samples, MgO crystallites grow in size from 160 to 250 Å for the Mg–Y–O system with the non-interacting constituents and, on the contrary, decrease in size from 215–250 Å to 150–200 Å for the Mg–La(Ce)–O systems with the interacting constituents. The reason for decreasing in size of the magnesia crystallizes in may be that the presence of La_2O_3–MgO or CeO_2–MgO solid solution in the Mg–La(Ce)–O systems prevents MgO crystallites from agglomeration.

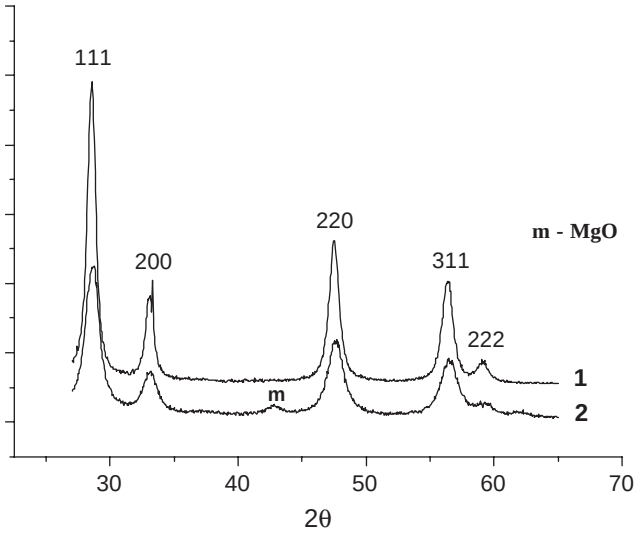

Fig. 1. XRD profiles of samples CeO_2 (1) and $(Ce,Mg)O_2$ (2) calcined in air at 450 °C for 4 h.

3.2. Textural properties

Surface area of the binary Mg–M–O systems under study is practically independent of the nature of M but depends mainly on the M content and T_{calc} value (Table 1). The surface area value for pure MgO prepared at the same pH and temperature as the binary systems and calcined at 450 °C is 220 $m^2 g^{-1}$. Addition of ca. 5 mol% M_2O_3 to MgO has only negligible effect on the specific surface area. An increase in the content of M_2O_3 in Mg–M–O systems from 5 to 23 mol% results in a decrease in the surface area from 210–240 to 100–110 $m^2 g^{-1}$ for the samples calcined at 450 °C. Increasing T_{calc} to 750 °C leads to the further decrease in the surface area value by a factor of 1.5–2.

As determined from N_2 adsorption isotherms measured at −196 °C, the binary Mg–M–O systems containing ≈5 mol% of M_2O_3, which were calcined at 450 °C possess a bimodal porous structure. The total volume and average diameter of pores decrease in the following series: Mg–Y–O (0.66 $cm^3 g^{-1}$; 161 Å) → Mg–La–O (0.50 $cm^3 g^{-1}$; 134 Å) → Mg–Ce–O (0.48 $cm^3 g^{-1}$; 115 Å).

3.3. Surface distribution and states of various elements in Mg– M–O systems

Table 2 presents E_b values of C1s, O1s and $M3d_{5/2}$ levels of the Mg–M–O samples containing ca. 5 mol% of

Table 2
Binding energies (E_b) of electron core levels and modified Auger parameters (α) determined for binary Mg–M–O (≈5 mol.% M_2O_3; M = Y, La, Ce) systems and their constituents

Sample[a]	E_b C1s (eV)	E_b O1s (eV)	E_b M3$d_{5/2}$ (eV)	α (eV)[b]
MgO	284.8 289.9	530.0 532.2	—	2485.1
Mg–Y–O	284.7 288.9	529.6 531.1	156.0	2484.8
Y_2O_3	284.7 289.2	528.9 531.3	156.8	—
Mg-La-O	284.9 289.4	529.4 531.5	833.8	2483.5
La_2O_3	284.9 289.3	529.0 531.4	834.4	—
Mg–Ce–O	284.6 289.0	529.4 531.4	881.1	2484.8
CeO_2	284.6 288.7	528.9 531.7	882.0	—

[a]All samples were pre-calcined in air at 450 °C for 4 h.
[b]$\alpha = E_b$ Mg1s + E_{kin} MgKLL.

M_2O_3 which were calcined at 450 °C. For comparison, E_b values of identical levels measured for the samples of pure MgO, $Y(La)_2O_3$ and CeO_2 which were prepared during this study are also given in Table 2. The surface atomic ratios determined for Mg–*M*–O by quantitative XPS method are presented in Table 3.

For Mg–*M*–O (≈5 mol% M_2O_3) systems, two C1*s* peaks at 284.6–284.9 and 288.9–289.4 eV are observed. The first peak is usually attributed to carbon impurity in the apparatus, and another one may be assigned to surface carbonate groups [21,22]. The XP spectra in the O1*s* region (Fig. 2) exhibit two intense peaks: one around 529.5 eV corresponding to lattice O^{2-} ions of MgO, the other at 531.1–531.5 eV corresponding likely to the surface hydroxyl and carbonate groups [23]. Both O1*s* peaks are shifted to lower E_b as compared with the spectrum of pure MgO ($E_b = 530.0$ and 532.2 eV for MgO). This shift may indicate that the effective negative charge on surface oxygen atoms in Mg–*M*–O systems is higher than in MgO i.e. surface O^{2-} ions in Mg–*M*–O are more basic than those in MgO. The O1*s* spectrum of Mg–La–O sample contains additionally two weak peaks at 522.1 and 524.7 eV (without charging correction using the internal standard E_b values of these peaks are 530.6 and 533.2 eV, respectively). Appearance of the additional peaks may be accounted for, e.g., by the non-uniform conductivity of Mg–La–O surface which involves regions of at least two types differing in conductivity and, correspondingly, in charging values.

Table 3
Surface atomic ratios determined by XPS for binary Mg–*M*–O (≈5 mol% M_2O_3; *M* = Y, La, Ce) systems

Sample[a]	Atomic ratios				Surface composition
	Mg/C[b]	O/Mg[c]	O/M[c]	*M*/Mg	
Mg–Y–O	6.6	1.58	9.2	0.172	$MgY_{0.17}O_{1.58}$
Mg–La–O	7.9	2.00	20.6	0.097	$MgLa_{0.1}O_2$
Mg–Ce–O	18.5	1.66	15.2	0.109	$MgCe_{0.11}O_{1.66}$

[a]All samples were pre-calcined in air at 450 °C for 4 h.
[b]The integral intensity of C1*s* peak at 288.9–289.4 eV related to surface carbonate species was only taken into account.
[c]The sum of integral intensities of O1*s* peaks at ~529.5 and 531–531.5 eV was taken into consideration.

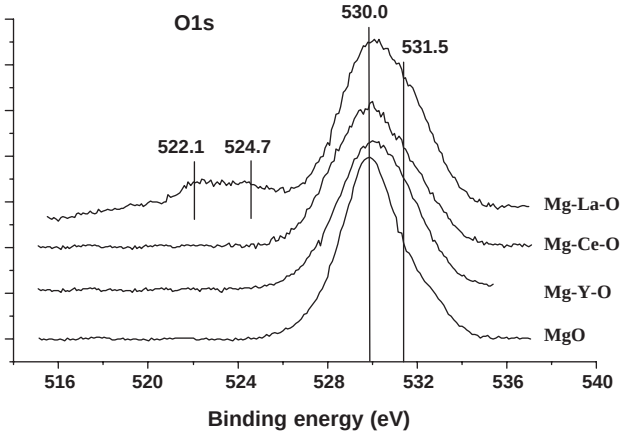

Fig. 2. O1*s* spectra of MgO and binary Mg–*M*–O (≈5 mol% M_2O_3) systems calcined in air at 450 °C for 4 h.

While the Mg2*s* peak position was used as the internal reference to calculate the charging value, the chemical state of magnesium in the Mg–*M*–O systems was estimated using a modified Auger parameter, α(Mg) which is the sum of E_b value of Mg1*s* core level and the kinetic energy of the corresponding Auger peak Mg*KLL* (the value of the Auger parameter is independent of the charging potential) [24]. As seen from Table 2, the value of α(Mg) obtained for Mg–Y(Ce)–O systems (2484.8 eV) are close to the known value for pure MgO (2485.1 eV), whereas the value of α(Mg) for Mg–La–O is lower by 1.6 eV than that of pure MgO. This difference indicates that the valency state and/or local environment of surface Mg atoms are different in Mg–La–O and MgO.

Fig. 3 comprises the spectra of Y3*d*, La3*d* and Ce3*d* core levels recorded for the Mg–*M*–O systems, which were calcined at 450 °C. The Y3*d* spectrum of binary Mg–Y–O system shown in Fig. 3A contains two overlapped peaks due to $Y3d_{5/2}$ and $Y3d_{3/2}$ transitions (as well as the spectrum of pure Y_2O_3). In the following the values of E_b will be referred to the more intense $Y3d_{5/2}$ peak. The value of E_b $Y3d_{5/2}$ (156.0 eV) is intermediate between the known data [25,26] for yttrium metal (155.5–156 eV) and pure Y_2O_3 (156–157 eV) (the sample of pure Y_2O_3 prepared by us exhibited the $Y3d_{5/2}$ peak at 156.8 eV). The surface Y/Mg atomic ratio determined by quantitative XPS equals 0.172 that are considerably higher than the bulk Y/Mg ratio of 0.078 as calculated from the chemical analysis data. Hence, it is reasonable to conclude that Mg–Y–O surface is enriched in yttrium. A surface enrichment in yttrium in combination with the shift of $Y3d_{5/2}$ peak by ≈1 eV to lower E_b values in the spectrum of Mg–Y–O sample relatively to the identical peak in the spectrum of pure Y_2O_3 suggest the presence of small-size yttrium oxide clusters at Mg–Y–O surface, the valency state of Y in these clusters being different from that in bulk Y_2O_3.

The La3*d* and Ce3*d* spectra of the Mg–La(Ce)–O systems (Fig. 3B and C), like the spectra of individual La_2O_3 and CeO_2, have a complex structure composed $La(Ce)3d_{5/2}$ and $La(Ce)3d_{3/2}$ peaks with their satellites. The main $La3d_{5/2}$ and $Ce3d_{5/2}$ peaks are observed at 833.8 and 881.1 eV, respectively, and shifted towards lower E_b values relatively, the corresponding features in the spectra of pure La_2O_3 and CeO_2 (E_b $La3d_{5/2} = 834.4$ eV, E_b $Ce3d_{5/2} = 882.0$ eV). The peaks observed in the Ce3*d* spectrum of the Mg–Ce–O sample may involve the contribution from Ce(III) ions which are usually contained in CeO_2 as an impurity [27]. While the satellite

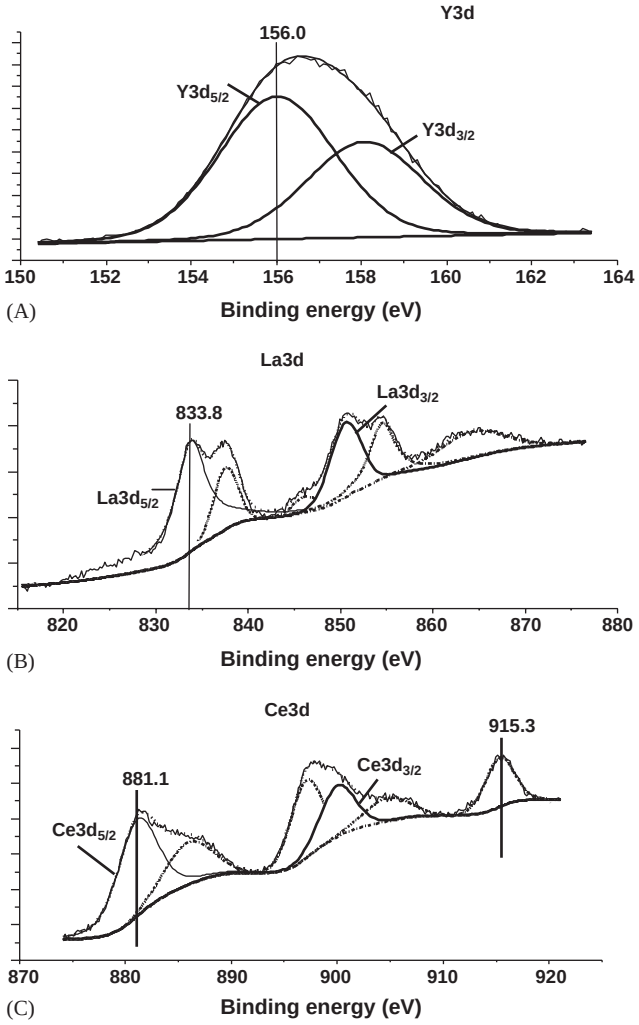

Fig. 3. M3*d* spectra of binary Mg–*M*–O (≈5 mol% M_2O_3) systems calcined in air at 450 °C: Mg–Y–O (A), Mg–La–O (B) and M–Ce–O (C). The satellite peaks are shown by dotted line.

Ce3$d_{3/2}$ peak at 915–917 eV arises only from Ce(IV) state, the relative intensity of this peak should be proportional to the Ce(III) content [28]. The corresponding estimation showed that the content of Ce(III) is ≈13% of the total cerium amount in the Mg–Ce–O sample. For the Mg–La(Ce)–O systems, the surface La/Mg and Ce/Mg ratios (Table 3) are noticeably higher than the related bulk ratios (La/Mg = 0.066 and Ce/Mg = 0.085). Hence, this is also the case when the surface of the binary oxide system is enriched in the lanthanide ions.

3.4. Acid–base properties of Mg–M–O surface

Fig. 4 shows IR spectra in the *v*(OH) region of MgO and binary Mg–*M*–O samples prepared at identical conditions. The spectrum of MgO exhibits an intense band at 3760 cm^{-1} and the broader absorption at lower frequencies (3550–3700 cm^{-1}). A sharp band at

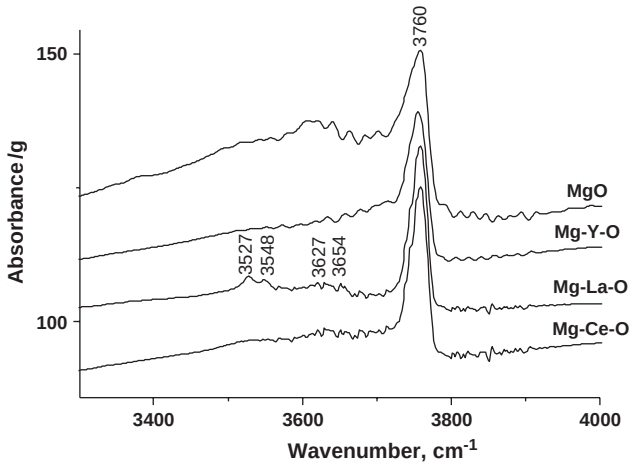

Fig. 4. FTIR spectra of OH groups located at the surface of MgO and binary Mg–*M*–O (≈5 mol% M_2O_3) systems calcined in air at 450 °C.

3760 cm^{-1} relates seemingly to the isolated OH groups located at edges and corners of MgO microcrystallites [29,30]. A broad band at ≈3600 cm^{-1} may be assigned to the OH groups located at {001} faces, which interacts by hydrogen bonds with their neighbors [31]. In the spectra of the binary Mg–*M*–O systems, the band related to isolated OH groups is observed at 3756 cm^{-1} regardless of the nature of *M*. The absorption at 3500–3700 cm^{-1}, which is characteristic of hydrogen-bonded OH groups, is considerably weaker in the spectra of the binary systems than in the spectrum of MgO. Very weak bands at 3525, 3550, 3627 and 3654 cm^{-1} are seen in the spectrum of Mg–La–O sample; they may be assigned to OH groups of surface bicarbonate species and to an impurity of $Mg(OH)_2$ [32].

The contents of isolated OH groups at MgO and Mg–*M*–O surface were calculated from the integral intensities of bands at 3760 and 3756 cm^{-1}, respectively. It was found that addition of lanthanide cations to MgO changes the surface content of isolated OH groups. The addition of ≈5 mol% of M_2O_3 to MgO increased the content of isolated OH groups from 180 to 220 μmol g^{-1} (if *M* is La or Ce), or decreased it to 160 μmol g^{-1} (if *M* is Y).

Fig. 5 presents IR spectra of MgO and Mg–*M*–O in the region of 1100–1700 cm^{-1}, which is characteristic of bond-stretching vibrations in surface carbonate and carboxylate species. The spectra of Mg–*M*–O samples contain intense overlapped bands at 1350–1550 cm^{-1}, which may be assigned to carbonate species formed through interaction of surface basic centers with atmospheric CO_2. The intensity of absorption at 1350–1550 cm^{-1} in the spectra of binary oxide systems decreases in the following series: Mg–Y–O > Mg–La–O > Mg–Ce–O. The complex structure of the spectra indicates the presence of several types of carbonate species on Mg–*M*–O surface. According to Ref. [32], the

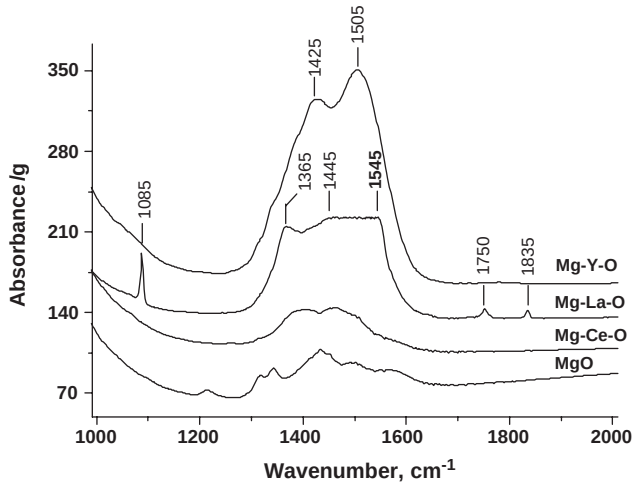

Fig. 5. FTIR spectra of carbonate species located at the surface of MgO and binary Mg–*M*–O (≈5 mol% M_2O_3) systems calcined in air at 450 °C.

bands at 1300–1600 cm^{-1} are characteristic of asymmetric $\nu(CO_3^{2-})$ vibrations of free carbonate ions (I) and monodentate carbonates (II)

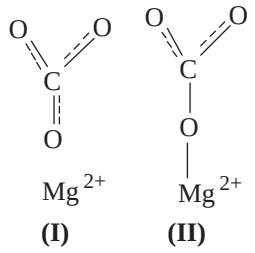

(I) **(II)**

which are typically produced if CO_2 reacts with strongly basic sites at the surface. Besides the bands at 1350–1550 cm^{-1}, the spectrum of Mg–La–O contains a weak sharp band at 1085 cm^{-1}, which may relate to symmetric $\nu(CO_3^{2-})$ vibrations, and the weak bands at 1750 and 1830 cm^{-1}. The 1750 cm^{-1} band may be assigned to ν (C═O) vibrations in bicarbonates formed due to interaction of CO_2 with surface hydroxyls, whereas the absorption at 1830 cm^{-1}, probably, associates with bridged carbonates containing metal–oxygen bonds of covalent nature [33]. The content of carbonates in Mg–*M*–O samples as estimated from integral intensity of absorption at 1350–1550 cm^{-1} varies from 900 to 3000 μmol g^{-1} in dependence on the nature of *M*. However, this is a very approximate estimation because the integral extinction coefficients of carbonate species are determined with a considerable error.

The IR spectrum of pure MgO in the 1300–1600 cm^{-1} region exhibits several weak heavily overlapped bands, which can hardly be assigned to certain surface carbonate species. The integral intensity of absorption at 1300–1600 cm^{-1} is far lower for MgO than for the binary systems, in particular, for Mg–Y–O and Mg–La–O. It is reasonable to conclude that the surface content of carbonate species is higher in Mg–*M*–O than in MgO and, hence, modification of the MgO surface with lanthanide ions results in a considerable increase in the amount of basic sites which are strong enough for interacting with CO_2 at room temperature.

In order to characterize surface acidity of the Mg–*M*–O systems, carbon monoxide capable of interacting with both Lewis and Broensted acid centers [19] was used as an IR probe molecule. The adsorption of CO onto surface acid sites causes positive C–O stretching frequency shift relatively the stretching frequency of CO in the gas–phase (2143 cm^{-1}), the C–O frequency shift, $\Delta\nu$(CO) being proportional to the strength of the acid centers. Fig. 6 shows IR spectra of CO adsorbed on Mg–*M*–O (≈5 mol% M_2O_3) at −196 °C and 10 Torr of CO. A single broad band at ca. 2150 cm^{-1} is observed for the all samples. The band may include the contributions of physically adsorbed CO (ν(CO) = 2140–2150 cm^{-1}), complexes of CO with very weak surface Lewis acid sites (ν(CO) = 2145–2155 cm^{-1}), and CO molecules that form hydrogen bonds with weakly acidic OH groups ($\nu_{CO} \approx 2160$ cm^{-1}). Based on the fact that the ν(OH) band at 3756 cm^{-1} is not perturbed upon CO adsorption on the binary systems, we concluded that the surface OH groups do not interact with CO, i.e. the OH groups on Mg–*M*–O surfaces do not possess a pronounced Broensted acidity. Hence, when CO is adsorbed on Mg–*M*–O, it may only interact with Lewis acidic sites representing the low-coordinate metal cations on the sample surface. However, it is impossible to determine content of these sites using the spectra recorded at the CO pressure as high as 10 Torr, because the contributions of physical CO adsorbtion and the interaction of CO with the weakest Lewis acidic sites cannot be correctly distinguished.

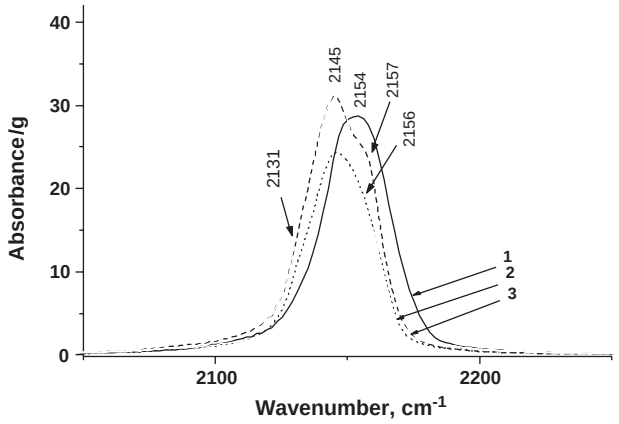

Fig. 6. FTIR spectra of CO adsorbed on binary Mg–*M*–O (≈5 mol% M_2O_3) systems at −196 °C and equilibrium pressure of 10 Torr: (1) Mg–Y–O, (2) Mg–La–O, (3) Mg–Ce–O. The spectra are recorded at −190 °C.

IR spectra of CO adsorbed on Mg–*M*–O (≈5 mol% M_2O_3) samples at −196 °C and a low CO pressure (0.1 Torr) are presented in Fig. 7. Under these conditions, the physical adsorption of CO is practically absent, and therefore the complexes of CO with various surface Lewis acidic sites can be more reliably identified. Table 4 comprises the IR frequencies of CO adsorbed on MgO and Mg–*M*–O surface, as well as the contents of surface Lewis acidic sites calculated from the integral intensities of related IR bands. In the spectra recorded at low CO pressure, the weak bands can be observed at 2200 cm^{-1} in the case of pure MgO and 2190–2196 cm^{-1} for binary Mg–*M*–O systems. These bands are typical for carbonyls formed with the comparatively strong Lewis acidic sites, such as 3-coordinated Mg^{2+} ions at the corners of MgO crystallites [34]. In the IR spectra recorded at the higher CO equilibrium pressure (Fig. 6), the bands at 2190–2200 cm^{-1} are not observed, probably, because $Mg^{2+}(CO)$ species are converted into dicarbonyls $Mg^{2+}(CO)_2$ characterized by a band at 2186 cm^{-1} which is masked by the intense absorption of physically adsorbed CO. The data obtained (Table 4) indicate a low surface content of strong Lewis acidic sites in MgO and Mg–*M*–O samples, which varies from 0.8 to 7.5 μmol g^{-1} in the following series: MgO < Mg–Ce–O < Mg–Y–O < Mg–La–O.

The IR spectra of CO adsorbed on MgO and Mg–La(Ce)–O samples at low CO pressure (Fig. 7) also contain the low frequency bands at 2163–2165 cm^{-1}. These bands arise from coordination of CO to the weaker Lewis acid sites, which may be four-coordinate Mg^{2+} ions at edges. After CO adsorption on Mg–Y–O, a band at 2177 cm^{-1}, which characterizes carbonyl complexes of Y^{3+} ions [35], appears instead of a 2163–2165 cm^{-1} band. In the spectrum of CO adsorbed on Mg–Ce–O sample, the band at 2177 cm^{-1} is seen as a shoulder of the 2165 cm^{-1} band. In this case a band at 2177 cm^{-1} can be presumably attributed to Ce^{4+}–CO complexes [35] (a band at 2123 cm^{-1} usually assigned to Ce^{3+}–CO complexes [36] is not observed in the spectrum). The surface content of weak Lewis acid sites as calculated from the integral intensity of 2165 cm^{-1} and/or 2177 cm^{-1} bands is much higher than that of strong Lewis acidic sites (ν(CO) = 2200–2190 cm^{-1}) and varies in the following series: MgO < Mg–Ce–O < Mg–La–O < Mg–Y–O (Table 4). The total content of surface Lewis acid sites in MgO and Mg–*M*–O samples varies the same way.

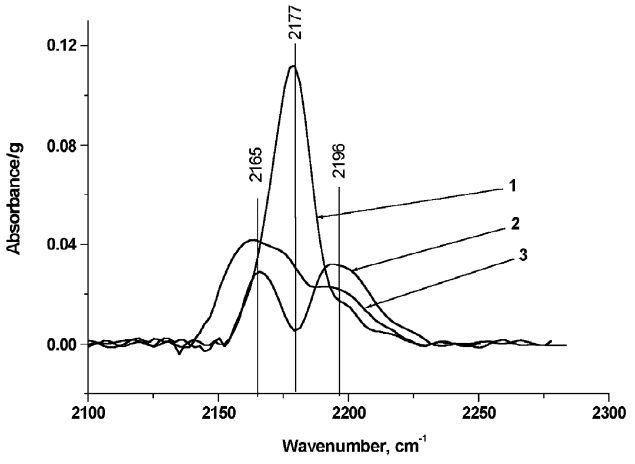

Fig. 7. FTIR spectra of CO adsorbed on binary Mg–*M*–O (≈5 mol% M_2O_3) systems at −196 °C and equilibrium pressure of 0.1 Torr: (1) Mg–Y–O, (2) Mg–La–O, (3) Mg–Ce–O. The spectra are recorded at −190 °C.

Table 4
Vibrational frequencies of CO (ν(CO)) adsorbed on MgO and binary Mg–*M*–O (≈5 mol.% M_2O_3; *M* = Y, La, Ce) systems and the content (N) of the related surface Lewis acid sites[a]

Sample[b]	Characteristics of surface Lewis acid sites		ΣN, μmol $(g)^{-1}$
	ν(CO), cm^{-1}	N, μmol $(g)^{-1}$	
MgO	2200	0.8	3.4
	2163	2.6	
Mg–Y–O	2190–2196	3.0	30
	2177	27	
Mg–La–O	2190–2196	7.5	22.5
	2165	15	
Mg–Ce–O	2190–2196	1.8	15
	2177	4.1	
	2165	9.1	

[a]Determined at −196 °C and 0.1 Torr of CO.
[b]All samples were pre-calcined in air at 450 °C for 4 h.

For probing surface basicity, deuterochloroform that forms H-bonded complexes with surface basic sites can be used as an IR probe molecule [19,37]. It has been established that the frequency value for the C–D stretching vibrations in $CDCl_3$ molecules decreases when the $CDCl_3$ vapor was adsorbed onto a matrix containing surface basic sites, the magnitude of the downward frequency shift [19] being correlated with the strength of basic sites. IR spectra of $CDCl_3$ adsorbed on MgO and Mg–*M*–O are shown in Fig. 8. The spectrum of pure MgO recorded after $CDCl_3$ adsorption demonstrates the bands at 2254, 2225 cm^{-1}, and a broad band at ≈2156 cm^{-1} derived from H-bonded complexes of $CDCl_3$ with weak, medium and strong basic sites, respectively. This observation agrees with the results of temperature-programmed desorption of CO_2 from MgO, which also indicate occurrence of basic sites of three types on MgO surface [38]. The weakest basic sites are supposed to be surface OH groups; the medium and strong sites are the low-coordinate O^{2-} ions located at different parts of MgO crystallites (at the edges and corners or at the {001} plane) [39]. When $CDCl_3$ is adsorbed on the Mg–*M*–O (≈5 mol% M_2O_3) surface, a

band with a maximum at 2229–2236 cm^{-1} is observed which is broadened at the low frequency side. Deconvolution of this band fits well by using three components at 2234–2240, 2210–2219 and 2166–2177 cm^{-1} (Fig. 8), which characterize H-complexes of $CDCl_3$ with weak, medium and strong basic sites, respectively. Wavenumbers of the ν(CD) bands of species formed by interaction of $CDCl_3$ with surface basic sites of MgO and Mg–*M*–O, as well as the contents of these sites are listed in Table 5. The total content of the surface basic sites varies as follows: MgO (1080 μmol g^{-1}) > Mg–La–O (680 μmol g^{-1}) > Mg–Ce–O (360 μmol g^{-1}) ≈ Mg–Y–O (330 μmol g^{-1}). The total concentration of surface basic sites measured for every Mg–*M*–O sample are higher than the total content of Lewis acidic sites on the surface of the same sample at least by a factor of 10–30. As seen from Table 5, the appearance of lanthanide ions on the MgO surface causes negative frequency shift of the bands at 2254 and 2225 cm^{-1}, which are typical for complexes of $CDCl_3$ with weak and medium basic sites, i.e. the basicity of these sites

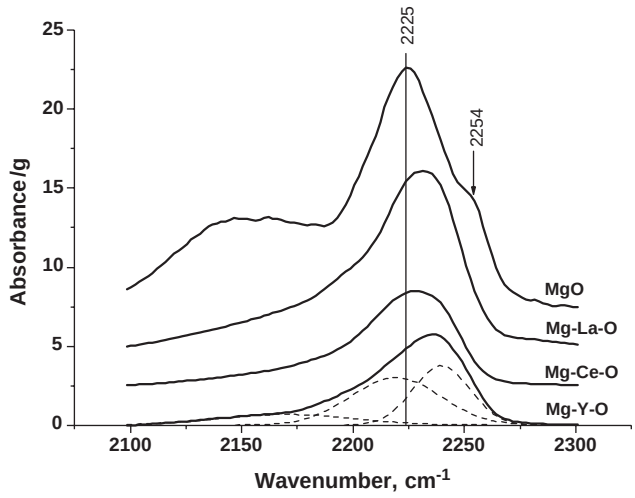

Fig. 8. FTIR spectra of $CDCl_3$ adsorbed on MgO and binary Mg–*M*–O (≈5 mol% M_2O_3) systems at 0 °C. The spectra are recorded at the same temperature. The dotted lines demonstrate the deconvolution of the spectrum of $CDCl_3$ adsorbed on Mg–Y–O sample into the individual components.

increases. On the contrary, the band at 2156 cm^{-1} derived from H-complexes of $CDCl_3$ with strongly basic sites is shifted by 10–20 cm^{-1} to higher values, the content of strong basic sites as determined from integral intensity of this band being decreased by a factor of 6–12 as compared with pure MgO. The fact that the modification of MgO surface with Y^{3+} or La^{3+} cations results in a dramatic decrease in the number of strong basic sites and their basicity seems unexpected one in view of the E_f values of the lanthanide cations added to MgO [11]. It is also in contrast with the data of IR spectroscopy of adsorbed CO_2 [40] demonstrating the preferable occurrence of strong basic sites on the surface of lanthanide oxides (such as La_2O_3 or Sm_2O_3), which are much stronger than the basic sites on the MgO surface. It is very likely that the strongest basic sites located at the surface of binary Mg–*M*–O systems actively interact with atmospheric CO_2 forming the surface carbonate species. Therefore, these sites may not be revealed by IR spectroscopy with acidic probe molecules like $CDCl_3$ at least when the evacuation treatment of a sample before the spectra registration is carried out at temperatures which are insufficiently high for carbonate decomposition. The sites are only detected in this case which are close in basicity to the sites at the MgO surface and react slowly with the atmospheric CO_2.

4. Conclusion

The study of binary oxide Mg–*M*–O (*M* = Y, La, Ce) systems prepared by co-precipitation technique has revealed that the interaction between the constituents with the formation of a solid solution occurs in the lanthanum- and cerium-containing systems but does not occur in the Mg–Y–O system. The difference in the phase composition appears to be responsible for the difference in the textural and surface properties of the prepared materials. In the Mg–La(Ce)–O systems the presence of the solid solutions prevents the MgO particles from aggregation. As a sequence, the crystallite size decreases with increasing in the content of La_2O_3 or

Table 5
Vibrational C–D frequencies (*v*(CD)) of $CDCl_3$ adsorbed on MgO and binary Mg–M–O (≈5 mol% M_2O_3; *M* = Y, La, Ce) systems and the content (*N*) of the related surface basic sites

Sample[a]	Surface basic sites					
	Weak		Medium		Strong	
	v(CD), cm^{-1}	*N*, μmol $(g)^{-1}$	*v*(CD) (cm^{-1})	*N* (μmol) $(g)^{-1}$	*v*(CD) (cm^{-1})	*N* (μmol) $(g)^{-1}$
MgO	2254	100	2225	580	2156	410
Mg–Y–O	2240	150	2219	150	2168	33
Mg–La–O	2235	385	2210	230	2166	65
Mg–Ce–O	2234	200	2212	105	2177	55

[a]All samples were pre-calcined in air at 450 °C for 4 h.

CeO_2 in the binary system. In the Mg–Y–O systems where the interaction between the constituents was not observed, MgO crystallites increase in size with the content of Y_2O_3. On the whole, the surface area of the Mg–*M*–O systems is practically independent of the nature of *M* but depends mainly on the *M* content and calcination temperature.

According to XPS data, the surface of the binary Mg–*M*–O systems is enriched in the lanthanide ions, the enrichment being most pronounced in the systems containing Y_2O_3. It is also shown that an effective negative charge on surface oxygen ions in Mg–*M*–O systems higher than in MgO, i.e. the basicity of surface O^{2-} ions in MgO modified with the lanthanide ions is higher than that in MgO itself. This effect is most pronounced in the case of La-containing systems.

FTIR spectroscopy data indicate the presence of Lewis acidic sites of several kinds, which may be coordinatively unsaturated Mg^{2+} and lanthanide ions at the Mg–M–O surface, but not Broensted acidity. The most of Lewis acid sites detected by FTIR are weak. The content of Lewis acid sites increases in the series of MgO < Mg–Ce–O < Mg–La–O < Mg–Y–O i.e. in the same order as the degree of Mg–*M*–O surface enrichment in a lanthanide cation. This correlation confirms that the increased Lewis acidity of Mg–*M*–O systems as compared with of MgO relates to the occurrence of lanthanide cationic centers at the oxide surface.

FTIR study also exhibits the presence of various basic sites at the Mg–*M*–O surface like at the MgO surface. Since the total concentration of surface basic sites is significantly exceeds that of surface Lewis acid sites in these materials, we may conclude the surfaces of binary Mg–*M*–O systems are overall basic like MgO surface. The modification of MgO with the lanthanide ions probably leads to an increase in strength of surface basic sites. However, the strongest basic sites at the Mg–*M*–O surface are blocked by carbonate species due to the interaction with atmospheric CO_2. In some studies of single and multi-component oxide systems e.g. in Ref. [41] the amount of CO_2 adsorbed on the material (or desorbed from it) is considered as a measure of surface basicity. Following this, we can suppose that the Mg–La–O samples with the highest content of surface carbonates are the most basic among the prepared Mg–*M*–O systems.

References

[1] K. Otsuka, K. Jinno, A. Morikawa, J. Catal. 100 (1986) 353.
[2] V.R. Choudhary, V.H. Rane, J. Catal. 130 (1991) 411.
[3] O.V. Krylov, Uspekhi Khimii 61 (1992) 1550 (in Russian).
[4] S.D. Jackson, G.J. Kelly, C.A. Hamilton, L. Davies, React. Kinet. Catal. Lett. 79 (2003) 213.
[5] G. Szollosi, M. Bartok, J. Mol. Catal., A: Chem. 418 (1999) 265.
[6] S. Murata, K Aika, J. Catal. 136 (1992) 110.
[7] M.S Khaja, Indian J. Chem. A. 32 (1993) 383.
[8] V.B. Shur, S.M. Yunusov, Izv. AN SSSR Ser. Khim. (5) (1998) 796 (in Russian).
[9] S.M. Yunusov, B.L. Moroz., A.S. Ivanova, V.A. Likholobov, V.B. Shur, J. Mol. Catal. A: Chem. 132 (1998) 263.
[10] K. Aika, K. Tamary, in: A. Nielsen (Ed.), Ammonia: Catalysis and Manufacture, Springer, Berlin, 1995, p. 104.
[11] K. Tanaka, A. Ozaki, J. Catal. 8 (1967) 1.
[12] W.J. Price, Analytical Atomic Absorption Spectrometry, Heyden, London, 1972.
[13] W. Kraus, G. Nolze, CPD Newslett. 20 (1988) 27.
[14] L.P. Solov'eva, S.V. Tsybulya, V.A. Zabolotnyi, "Polycrystal" software package for structural analysis, Boreskov Institute of Catalysis, Novosibirsk, 1988 (in Russian).
[15] ASTM, Diffraction Data Cards and Alphabetical and Grouped Numerical Index of X-ray Diffraction Data, ASTM, Philadelphia, 1967.
[16] J.I. Langford, J. Appl. Cryst. 1 (1978) 22.
[17] Ya.S. Umanskii, Radiography of Metals, Metallurgiya, Moscow, 1970, p. 273 (in Russian).
[18] D.A. Shirley, Phys. Rev. B 5 (1972) 4709.
[19] E.A. Paukshtis, IR Spectroscopy in Heterogeneous Acid-base Catalysis, Nauka, Nowosibirsk, 1992 (in Russian).
[20] N.E. Buyanova, A.P. Karnaukhov, Yu.A. Alabuzhev, Determination of Surface Area of Dispersed and Porous Materials, Institute of Catalysis, Novosibirsk, 1978 (in Russian).
[21] T. Grzybek, M. Baerns, J. Catal. 129 (1991) 106.
[22] R. Mariscal, J. Soria, M.A. Pena, J.L.G. Fierro, J. Catal. 147 (1994) 535.
[23] R. Mariscal, M.A. Pena, J.L.G. Fierro, Appl. Catal. A: General 131 (1995) 243.
[24] V.I. Bukhtiyarov, I.P. Prosvirin, R.I. Kvon, J. Electron. Spectrosc. Relat. Phenom. 77 (1996) 7.
[25] C.D. Wagner, W.M. Riggs, L.E. Davis, J.F. Moulder, G.E. Muilenberg, Handbook of X-ray Photoelectron Spectroscopy, Perkin-Elmer, Eden Prairie, MN, 1979.
[26] D.R. Mullins, S.H. Overbury, D.R. Hantley, Surf. Sci. 409 (1998) 307.
[27] M.Yu. Smirnov, G.W. Graham, Catal. Lett. 72 (2001) 39.
[28] C. Martin, I. Martin, V. Rives, J. Mol. Catal. 73 (1992) 51.
[29] G. Szollosi, M. Bartok J. Mol. Struct. 482–483 (1999) 13.
[30] S. Coluccia, L. Marchese, S. Lavagnino, M. Anpo, Spectroch. Acta 43A (1987) 1573.
[31] K. Nakamoto, Infrared and Raman Spectra of Inorganic and Coordination Compounds, Wiley, New York, 1986.
[32] A.A. Davydov, M.L. Shepotko, A.A. Budneva, Catal. Today 24 (1995) 225.
[33] Ya.M. Grigor'ev, D.V. Pozdnyakov, V.N. Filimonov, J. Phiz. Khim. 46 (1972) 316.
[34] M.I. Zaki, B. Vielhaber, H. Knozinger, J. Phys. Chem. 90 (1986) 3176.
[35] K.I. Hadjiivanov, G.N. Vayssilov, in: B.C. Gates, H. Knoezinger (Eds.), Advances in Catalysis, Vol. 47, Elsevier, San Diego (USA), 2002, p. 308.
[36] E.A. Paukshtis, N.S. Kotsarenko, L.G. Karakchiev, React. Kinet. Catal. Lett. 12 (1979) 315.
[37] R.I. Soltanov, E.A. Paukshtis, E.N. Yurchenko, React. Kinet. Catal. Lett. 23 (1983) 333.
[38] S. Kus, M. Otremba, A. Torz, M. Taniewski, Appl. Catal. A: General 230 (2002) 263.
[39] A. Zecchina, S. Collucia, C. Morterra, Appl. Spectrosc. Rev. 21 (1985) 259.
[40] P. Rosynek, D.T. Magnuson, J. Catal. 48 (1977) 417.
[41] L. Yu, W. Li, V. Ducarme, C. Mirodatos, G.A. Martin, Appl. Catal. A: General 175 (1998) 173.